Journal of Alloys and Compounds 507 (2010) 84–92

Contents lists available at ScienceDirect

Journal of Alloys and Compounds

journal homepage: www.elsevier.com/locate/jallcom

Thermodynamic assessment of the Cr–Mn–O system

Lina Kjellqvist*, Malin Selleby

Materials Science and Engineering, KTH, SE-100 44 Stockholm, Sweden

ARTICLE INFO

Article history:
Received 14 August 2009
Received in revised form 21 April 2010
Accepted 25 April 2010
Available online 19 June 2010

Keywords:
Thermodynamic modelling
CALPHAD
Cr–Mn–O system

ABSTRACT

The C–Cr–Fe–Ni–O and Fe–Mn–O systems have been studied earlier with the aim to thermodynamically describe the influence of oxygen on high alloyed steels. In this study the ternary Cr–Mn–O system is assessed. The liquid phase is described using the ionic two-sublattice model. Good agreement between calculated and experimental values is achieved.

1. Introduction

In the present study a new ternary, Cr–Mn–O, is added to the description of the C–Cr–Fe–Ni–O system [1,2]. In parallel, the Fe–Mn–O and Mn–Ni–O systems are being assessed [3,4] and in combination they will yield a consistent thermodynamic database for the C–Cr–Fe–Mn–Ni–O system. That system is of fundamental importance when describing the influence of oxygen on high alloyed steels. The solid phases are of interest as material in the interconnects in solid oxide fuel cells (SOFC). Ferritic steels have been considered as interconnect materials of SOFCs with operating temperatures in the range 873–1073 K. Recent studies have shown that the oxide scale formed on ferritic interconnects primarily are composed of Cr_2O_3 and $(Cr, Mn)_3O_4$ spinel [5–7]. A thermodynamic description of the Fe–Cr–Mn–O system could thus be of invaluable help to understand the oxidation behaviour of such interconnects. Other important areas are oxidation processes like the formation of oxide layers on high alloyed steels, inner oxidation, sintering processes and high temperature corrosion. The liquid phase is of interest for e.g. the interaction between steel and its slag in a metallurgical context.

This work will also contribute to the development of a larger oxide database by which it will be possible to treat many types of different steels. The models in this work are compatible with the models used in a parallel work on the Al_2O_3–CaO–Fe–O–MgO–SiO_2 system [8,9]. The database can be used with appropriate thermodynamic software, e.g. Thermo-Calc [10], to calculate thermodynamic properties, equilibrium states and phase diagrams. The thermodynamic database can also be combined with a kinetic database and suitable software, e.g. Dictra, to simulate diffusion controlled phase transformations where oxides play an important role [11]. The description of the constituent binaries Cr–Mn [12], Mn–O [3,13] and Cr–O [14] are combined to form the ternary and the model parameters for the Cr–Mn–O system are optimised using experimental data available in the literature.

Cr–Mn–O has been assessed recently by both Jung [15] and by Povoden et al. [16], but is reassessed in this work. Except for the Mn–O description that Povoden et al. also used, they both based their assessments on other descriptions for the binary subsystems than the ones used in the present work. Furthermore, the description of the spinel phases is more ambitious in the present work. Povoden et al. [16] used a stoichiometric description unable to describe the cation distribution between tetrahedral and octahedral sites. Jung [15] did not describe the deviation from stoichiometry towards the metallic side for Cr_3O_4, $MnCr_2O_4$ and Mn_3O_4. An extensive thermodynamic database for the Al_2O_3–CaO–CoO–CrO–Cr_2O_3–FeO–Fe_2O_3–MgO–MnO–NiO–SiO_2 system has been developed by Decterov et al. [17] using the modified quasichemical model [18–20] to describe the molten slag phase. Those assessments are not considered in the present work since the two liquid models are not compatible.

2. Thermodynamic models

2.1. Liquid

The ionic two-sublattice liquid model [21,22] is applied to the Cr–Mn–O system, using the formula $(Cr^{+2}, Mn^{+2})_P(O^{-2}, Va^{-Q}, CrO_{1.5}, MnO_{1.5})_Q$. The liquid phase in the Fe–O system was first modelled with $(Fe^{+2}, Fe^{+3})_P(O^{-2}, Va^{-Q})_Q$[23], but later Fe^{+3} was

---

* Corresponding author.
E-mail address: lina@mse.kth.se (L. Kjellqvist).

0925-8388/$ – see front matter © 2010 Elsevier B.V. All rights reserved.
doi:10.1016/j.jallcom.2010.04.252

replaced by a neutral species, $FeO_{1.5}$[24]. This change was imposed by an equivalent change for Al-containing system where Al^{+3} was replaced by $AlO_{1.5}$ in order to better control the unwanted reciprocal miscibility gaps that occurred in e.g. Al_2O_3–CaO–SiO_2. However, even though a new model for liquid Al_2O_3 (without $AlO_{1.5}$) has been developed [25], the $FeO_{1.5}$ species has been kept. To conform to the model in Fe–O, neutral $CrO_{1.5}$ and $MnO_{1.5}$ species are used to model liquid Cr_2O_3 and Mn_2O_3 in the present work. Cr–O was earlier assess by Taylor and Dinsdale [26], who only used only one oxidation state of Cr to model the liquid phase, namely Cr^{+3}. The liquid phase in Cr–O is reassessed in a parallel work [14] using the formula $(Cr^{+2})_P(O^{-2}, Va^{-Q}, CrO_{1.5})_Q$. It has been established that Cr is mainly divalent in liquid oxide at low oxygen potentials and Cr^{+2} is a prerequisite in the model if calculations of redox equilibria of liquid oxide should be possible.

P and Q are the number of sites on each sublattice. P and Q vary so that electroneutrality is maintained. The same model can be used both for metallic and oxide melts. At low levels of oxygen, the model becomes equivalent to a substitutional solution model between metallic atoms. The ionic two-sublattice model was developed within the framework of the compound energy formalism (CEF) [27], which is used to describe phases using two or more sublattices and is widely used in Calphad assessments [28,29]. The Gibbs energy of the liquid phase is expressed by:

$$\begin{aligned} G_m = {} & y_{Cr^{+2}} y_{O^{-2}} {}^{o}G_{Cr^{+2}:O^{-2}} + y_{Mn^{+2}} y_{O^{-2}} {}^{o}G_{Mn^{+2}:O^{-2}} \\ & + Q y_{Va^{-Q}} (y_{Cr^{+2}} {}^{o}G_{Cr^{+2}:Va^{-Q}} + y_{Mn^{+2}} {}^{o}G_{Mn^{+2}:Va^{-Q}}) \\ & + Q(y_{CrO_{1.5}} {}^{o}G_{CrO_{1.5}} + y_{MnO_{1.5}} {}^{o}G_{MnO_{1.5}}) + RTP(y_{Cr^{+2}} \ln(y_{Cr^{+2}}) \\ & + y_{Mn^{+2}} \ln(y_{mn^{+2}})) + RTQ(y_{O^{-2}} \ln(y_{O^{-2}}) + y_{Va^{-Q}} \ln(y_{Va^{-Q}}) \\ & + y_{CrO_{1.5}} \ln(y_{CrO_{1.5}}) + y_{MnO_{1.5}} \ln(y_{MnO_{1.5}})) + {}^{E}G_m \end{aligned} \tag{1}$$

where y denotes the site fraction and ${}^{E}G_m$ is the excess Gibbs energy which depends on the interaction between species within each sublattice:

$$\begin{aligned} {}^{E}G_m = {} & Q y_{Va}^2 y_{Cr^{+2}} y_{Mn^{+2}} ({}^{0}L_{Cr^{+2},Mn^{+2}:Va} + {}^{1}L_{Cr^{+2},Mn^{+2}:Va}(y_{Mn^{+2}} - y_{Cr^{+2}})) \\ & + y_{Va} y_{Cr^{+2}} y_{O^{-2}} ({}^{0}L_{Cr^{+2}:O^{-2},Va} + {}^{1}L_{Cr^{+2}:O^{-2},Va}(y_{O^{-2}} - y_{Va})) \\ & + y_{Va} y_{Mn^{+2}} y_{O^{-2}} ({}^{0}L_{Mn^{+2}:O^{-2},Va} + {}^{1}L_{Mn^{+2}:O^{-2},Va}(y_{O^{-2}} - y_{Va})) \\ & + y_{Cr^{+2}} y_{O^{-2}} y_{CrO_{1.5}} {}^{0}L_{Cr^{+2}:O^{-2},CrO_{1.5}} \\ & + y_{Mn^{+2}} y_{O^{-2}} y_{MnO_{1.5}} {}^{0}L_{Mn^{+2}:O^{-2},MnO_{1.5}} \\ & + y_{Cr^{+2}} y_{CrO_{1.5}} {}^{0}L_{Cr^{+2}:CrO_{1.5},Va} + y_{Cr^{+2}} y_{MnO_{1.5}} {}^{0}L_{Cr^{+2}:MnO_{1.5},Va} \\ & + y_{Mn^{+2}} y_{CrO_{1.5}} {}^{0}L_{Mn^{+2}:CrO_{1.5},Va} + y_{Mn^{+2}} y_{MnO_{1.5}} {}^{0}L_{Mn^{+2}:MnO_{1.5},Va} \end{aligned} \tag{2}$$

Above only the interaction parameters that are actually used in the present work are included. A colon is used to separate species on different sublattices and a comma is used to separate species on the same sublattice.

2.2. Spinel: cubic and tetragonal

There are two types of spinel phases in the Cr–Mn system; cubic and tetragonal spinels (Strukturbericht $H1_1$ for cubic spinel). Hausmannite (Mn_3O_4) is a tetragonal spinel (α-Mn_3O_4) at low temperatures and transforms to a cubic spinel (β-Mn_3O_4) at higher temperatures. α-Mn_3O_4 dissolves small amounts of Cr, while β-Mn_3O_4 extend up to $MnCr_2O_4$. Cr_3O_4 is also a cubic spinel and is included in the same model. Only under some conditions: high temperature and low oxygen partial pressure, is the cubic spinel stable in the composition range $MnCr_2O_4$–Cr_3O_4. The tetragonal distortion originates from the Jahn–Teller distortion of octahedral sites occupied by Mn^{+3} ions. The modelling of the spinel phase is discussed in detail in previous works [1,3,30].

In accordance with the work by Dorris and Mason [31], it is assumed that α- and β-spinel have different ionic configurations: α-spinel is described by $(Cr^{+2}, Cr^{+3}, Mn^{+2}, Mn^{+3})_1(Cr^{+3}, Mn^{+2}, Mn^{+3}, Va)_2(Cr^{+2}, Mn^{+2}, Va)_2(O^{-2})_4$ and β-spinel by $(Cr^{+2}, Cr^{+3}, Mn^{+2})_1(Cr^{+3}, Mn^{+2}, Mn^{+3}, Mn^{+4}, Va)_2(Cr^{+2}, Mn^{+2}, Va)_2(O^{-2})_4$. The first sublattice represents tetrahedral sites and the second sublattice represents octahedral sites. A normal spinel has the divalent ions on the tetrahedral sites and the trivalent ions on the octahedral sites. An inverse 23-spinel has trivalent ions on the tetrahedral sites and divalent and trivalent ions on the octahedral sites, while an inverse 42-spinel has divalent ions on the tetrahedral sites and divalent and tetravalent ions on the octahedral sites.

The models for the spinel phases might seem a bit complicated at first sight, why an explanation for this complex approach is in place. α- and β-Mn_3O_4 are modelled with vacancies on the octahedral sublattice and an extra interstitial sublattice, with Mn^{+2} in places that are normally filled with vacancies, to be able to model the deviation from stoichiometry according to the experiments from Keller and Dieckmann [32]. According to Dorris and Mason the degree of inversion of Mn_3O_4 remains small even at high temperature. It would be expected to be even smaller at lower temperature, i.e. smaller in α-Mn_3O_4 than in β-Mn_3O_4. Mn^{+3} would thus be unnecessary to include on the tetrahedral sublattice of α-Mn_3O_4. But Mn^{+3} on the tetrahedral sublattice in α-Mn_3O_4 are needed to be able to retain electroneutrality when octahedral vacancies are included to describe the deviation from stoichiometry towards the oxygen-side. Cr^{+3} on the tetrahedral sublattice might seems unnecessary to include because the degree of inversion of $MnCr_2O_4$ is very low, but for this description to be consistent with the description of the Fe–Cr–Ni–O spinel in an earlier work [1] were Cr^{+3} is present on the tetrahedral sublattice, Cr^{+3} must be included also here. Cr^{+2} in the interstitial sublattice also originate from the Fe–Cr–Ni–O assessment, where it is needed to describe the oxygen activity dependence in $(Cr_xFe_{1-x})_{3-\delta}O_4$.

The number of end-members for the α- and β-spinels are 48 and 45 respectively and most of these have a net charge and can be present only in neutral combinations, but each end-member must be given a Gibbs energy value. In practice the number of independent parameters is much less than this. In the models above only four independent parameters are used to model hausmannite, one for Cr_3O_4, two for $MnCr_2O_4$ and one for interstitial Cr^{+2}. The 48 and 45 end-members in α- and β-spinel are thus reduced to 8 model parameters for each phase. For the remaining parameters, simple relationships are assumed to hold for the substitution of one cation for another on the same lattice, for example:

$$G_{Cr^{+2}:Cr^{+3}} - G_{Cr^{+3}:Cr^{+3}} = G_{Cr^{+2}:Mn^{+3}} - G_{Cr^{+3}:Mn^{+3}} \tag{3}$$

i.e. substitution of a Cr^{+2} for a Cr^{+3} on the first sublattice is assumed to be independent of which ions reside on the other lattices. The relationship in Eq. (3) is a so called reciprocal reaction, and can be rearranged as:

$$\begin{aligned} \Delta G_{Cr^{+2},Cr^{+3}:Mn^{+3},Cr^{+3}} = {} & G_{Cr^{+2}:Cr^{+3}} - G_{Cr^{+3}:Cr^{+3}} - G_{Cr^{+2}:mn^{+3}} \\ & + G_{Cr^{+3}:Mn^{+3}} = 0 \end{aligned} \tag{4}$$

Proceeding in this way allows all end-members to be evaluated based on the 8 model parameters mentioned above. The model is thus rather simple in all its complexity and extrapolations into higher-order systems are shown to give accurate results [33] in the Fe–Cr–Mn–Ni–O system.

Cr has a low solubility in α-spinel. Below, the description on the modelling is focused on the cubic phase, but most parts of the

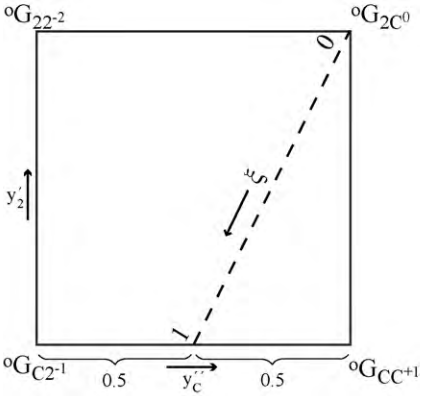

Fig. 1. Compositional square for $MnCr_2O_4$. The possible neutral compositions are on the marked neutral line.

discussion hold for both phases. Many parameters in the tetragonal α-spinel have the same functions as the cubic β-spinel.

$MnCr_2O_4$ is described using $(Cr_{\xi}{}^{+3}, Mn_{1-\xi}{}^{+2})(Cr_{2-2\xi}{}^{+3}, Mn_{2\xi}{}^{+2})(O^{-2})_4$, where ξ is the inversion parameter. In $MnCr_2O_4$, the degree of inversion is very low, hence $MnCr_2O_4$ is a normal spinel, $\xi = 0$. The four ^oG parameters ($^oG^{\beta}_{Cr^{+3}:Cr^{+3}}$, $^oG^{\beta}_{Mn^{+2}:Mn^{+2}}$, $^oG^{\beta}_{Mn^{+2}:Cr^{+3}}$ and $^oG^{\beta}_{Cr^{+3}:Mn^{+2}}$) are from now on denoted $^oG^{\beta}_{CC}$, $^oG^{\beta}_{22}$, $^oG^{\beta}_{2C}$ and $^oG^{\beta}_{C2}$. The Gibbs energy of stoichiometric β-$MnCr_2O_4$ is given by

$$^oG^{\beta}_m = y'_2y''_2{}^oG^{\beta}_{22} + y'_2y''_C{}^oG^{\beta}_{2C} + y'_Cy''_2{}^oG^{\beta}_{C2} + y'_Cy''_C{}^oG^{\beta}_{CC} - TS_m + {}^EG_m \quad (5)$$

where the superscripts ′ and ″ denote tetrahedral and octahedral sites, respectively. This is a system with a neutral line between the $^oG^{\beta}_{2C}$ corner and the $^oG^{\beta}_{CC}$–$^oG^{\beta}_{C2}$ side, see Fig. 1. All points on the neutral line between the normal and inverse spinels represent the stoichiometric composition, but with different distributions of ions on the tetrahedral and octahedral sublattices. Only one point on the line represents the equilibrium composition at a given temperature. The site fractions in Eq. (5) could be replaced by the variable describing the disorder, $\xi = y'_3 = 1 - y'_2 = 2 - 2y''_3 = 2y''_2$. $\xi = 0$ yields the normal state $(Mn^{+2})_1(Cr^{+3})_2$ and $\xi = 1$ yields the inverse state $(Cr^{+3})_1(Cr_{0.5}{}^{+3}, Mn_{0.5}{}^{+2})_2$. The excess energy, ^EG_m, in Eq. (5) should be neglected since there already are more compound energies than experimental information. Rearranging Eq. (5) and expressing all site fractions in terms of ξ yields:

$$G^{\beta}_m + TS_m(\xi) = {}^oG^{\beta}_{2C} + J^{\beta}_{2C}\xi + 0.5\Delta G^{\beta}_{2C:2C}\xi^2 \quad (6)$$

$$\Delta G^{\beta}_{2C:2C} = {}^oG^{\beta}_{2C} + {}^oG^{\beta}_{C2} - {}^oG^{\beta}_{22} - {}^oG^{\beta}_{CC} \quad (7)$$

$$J^{\beta}_{2C} = {}^oG^{\beta}_{CC} + 0.5{}^oG^{\beta}_{22} - 1.5{}^oG^{\beta}_{2C} \quad (8)$$

Since the degree of inversion is low, the Gibbs energy of β-$MnCr_2O_4$ is given by $^oG^{\beta}_{2C}$. $^oG^{\beta}_{22}$ and $^oG^{\beta}_{CC}$ are fixed from the assessments of the Mn–O and Cr–O systems, respectively. J^{β}_{2C} is used to model the degree of inversion. If $^oG^{\beta}_{22}$ and $^oG^{\beta}_{CC}$ were not already known, we would have chosen one of them as a reference and the other one would be used to model the degree of inversion. The last parameter ($^oG^{\beta}_{C2}$), would be obtained by giving some value for the reciprocal relation, $\Delta G^{\beta}_{2C:2C}$. The established value in the model for the spinel phase is $\Delta G^{\beta}_{2C:2C} = 0$. Since $^oG^{\beta}_{22}$ and $^oG^{\beta}_{CC}$ are known, J^{β}_{2C} and $\Delta G^{\beta}_{2C:2C}$ could not both be evaluated. Since no detailed studies on the cation distribution are available, $\Delta G^{\beta}_{2C:2C} = 0$ is chosen. This choice will give an almost perfectly normal spinel for all temperatures.

To be able to model the spinel all the way to Mn_3O_4 and also include Cr_3O_4 in the same model, Cr^{+2} should be included on the tetrahedral sublattice and Mn^{+3} and Mn^{+4} on the octahedral sublattice. This give, besides $^oG^{\beta}_{cC}$ ($^oG^{\beta}_{Cr^{+2}:Cr^{+3}}$), $^oG^{\beta}_{23}$ ($^oG^{\beta}_{Mn^{+2}:Mn^{+3}}$) and $^oG^{\beta}_{24}$ ($^oG^{\beta}_{Mn^{+2}:Mn^{+4}}$) known from the Cr–O and Mn–O assessments, five more unknown parameters: $^oG^{\beta}_{C3}$, $^oG^{\beta}_{C4}$, $^oG^{\beta}_{c2}$, $^oG^{\beta}_{c3}$ and $^oG^{\beta}_{c4}$, which we evaluate from the reciprocal relations $\Delta G_{C2:23} = 0$, $\Delta G_{C2:24} = 0$, $\Delta G_{c2:C2} = 0$, $\Delta G_{c2:C3} = 0$ and $\Delta G_{c2:C4} = 0$. β-Mn_3O_4 shows a small deviation from stoichiometry. Vacant sites are formed in the octahedral sublattice to model the deviation towards oxygen in equilibrium with Mn_2O_3. To model deviation towards manganese in equilibrium with halite, Mn^{+2} is assumed to enter interstitial sites normally filled with vacancies. Cr^{+2} ions are also allowed on the interstitial sublattice, this originates from the modification of the Cr–Fe–O assessment [1]. The final model for the Cr–Mn spinel is $(Cr^{+2}, Cr^{+3}, Mn^{+2})_1(Cr^{+3}, Mn^{+2}, Mn^{+3}, Mn^{+4}, Va)_2(Cr^{+2}, Mn^{+2}, Va)_2(O^{-2})_4$.

The $^oG^{\beta}_{Mn^{+2}:Cr^{+3}:Mn^{+2}:O^{-2}}$-parameter was used as a model parameter. Without this parameter a Cr–Mn-spinel with some (≈1%) interstitial Mn is formed, preventing the experimental data on the phase boundary β-spinel/halite to be reproduced. The 21 remaining parameters in the nonstoichiometric system ($^oG^{\beta}_{cC2}$, $^oG^{\beta}_{CC2}$, $^oG^{\beta}_{cV2}$, $^oG^{\beta}_{CV2}$, $^oG^{\beta}_{2MC}$ ($M = Mn^{+2}, Mn^{+3}, Mn^{+4}$, Va), $^oG^{\beta}_{NM*}$ ($N = Cr^{+2}, Cr^{+3}$, $M = Mn^{+2}, Mn^{+3}, Mn^{+4}$, $* = Cr^{+2}, Mn^{+2}$), $^oG^{\beta}_{2CC}$) are evaluated using reciprocal reactions, see Eq. (4).

Mn_3O_4 and $MnCr_2O_4$ undergo magnetic transitions at low temperatures (∼40 K). The transition in $MnCr_2O_4$ is not considered in this work due to the low temperature at which it takes place. The Curie temperature of Mn_3O_4 is modelled to be able to describe how the Curie temperature varies in Fe_3O_4–Mn_3O_4 in the Fe–Mn–O assessment [3]. The magnetic contribution to the Gibbs energy is given by a model proposed by Inden [34] and adapted by Hillert and Jarl [35].

2.3. Manganosite, bixbyite, eskolaite and pyrolusite

The manganosite (MnO) phase has the NaCl-type structure (Strukturbericht B1), with the generic name halite. The halite phase is described using a model within the CEF with two sublattices; one for metal ions and one for oxygen ions. MnO has a considerable solid solubility, due to the oxidation of Mn^{+2} to Mn^{+3} and the formation of cation vacancies. The solubility of Cr in manganosite is modelled with Cr^{+3} ions on the metallic sublattice. The phase is thus represented as:

$(Cr^{+3}, Mn^{+2}, Mn^{+3}, Va)_1(O^{-2})_1$

The parameter $G^{\text{halite}}_{Cr^{+3}:O^{-2}}$ is evaluated in the Cr–Fe–O assessment [36], and the solubility of Cr in manganosite is obtained using an interaction parameter, $^0L^{\text{halite}}_{Cr^{+3},Mn^{+2}:O^{-2}}$. α-bixbyite (α-$Mn_2O_3$) transforms to β-$Mn_2O_3$ (Strukturbericht $D5_3$) at around 300 K. The α-modification was not considered in this work due to the low transformation temperature. The solubility of Cr in β-bixbyite is modelled by adding Cr^{+3} ions on the cation sublattice. The model yields:

$(Mn^{+3}, Cr^{+3})_2(O^{-2})_3$

Eskolaite (Cr_2O_3) has the generic name corundum (Strukturbericht $D5_1$). The solubility of Mn in eskolaite is modelled by adding Mn^{+3} ions on the cation sublattice. The model becomes:

$(Cr^{+2}, Cr^{+3}, Mn^{+3})_2(Cr^{+3}, Va)_1(O^{-2})_3$

The parameter $G^{\text{corundum}}_{\text{Mn}^{+3}:\text{Va}:\text{O}^{-2}}$ is evaluated in the Fe–Mn–O assessment [3], and the solubility of Mn in eskolaite is obtained using an interaction parameter, ${}^{0}L^{\text{corundum}}_{\text{Cr}^{+3},\text{Mn}^{+3}:\text{Va}:\text{O}^{-2}}$.

Pyrolusite (MnO_2) with the generic name rutile (Strukturbericht C4) is described as a stoichiometric phase. There are no reports on any solubility of Cr in pyrolusite.

The description of Cr_2O_3 is taken from Taylor and Dinsdale [26] and the descriptions of MnO, β-Mn_2O_3 and MnO_2 are all from Grundy et al. [13].

3. Experimental data

There are very few studies on the thermodynamic properties of $MnCr_2O_4$. No heat capacity measurements were performed, and the enthalpy and entropy at 298 K is not known. Several values for the Gibbs energy of formation of $MnCr_2O_4$ ($\Delta G^f_{MnCr_2O_4}$) from MnO and Cr_2O_3 are published. The most recent investigation is from Tanahashi et al. [37] who derived $\Delta G^f_{MnCr_2O_4} = -59 \pm 8$ kJ/mol at 1873 K by equilibrating molten iron or copper with an MnO-saturated $MnCr_2O_4$ crucible. $\Delta G^f_{MnCr_2O_4}$ was calculated using the compiled ΔG^f_{MnO} and $\Delta G^f_{Cr_2O_3}$ from Barin [38].

Tsai and Muan [39] reported $\Delta G^f_{MnCr_2O_4}$ from MnO and Cr_2O_3 at 1773 and 1873 K, calculated from the reaction

$$CrO_{1.5} + Mn_{0.5}AlO_2 = AlO_{1.5} + Mn_{0.5}CrO_2 \tag{9}$$

They achieved $\Delta G^f_{MnCr_2O_4} = \Delta G^f_{MnAl_2O_4} - 20,000$ at 1873 K and $\Delta G^f_{MnCr_2O_4} = \Delta G^f_{MnAl_2O_4} - 19,200$ at 1773 K. The result will depend on which value is chosen for $\Delta G^f_{MnAl_2O_4}$. In their calculations they used $\Delta G^f_{MnAl_2O_4}$ at 1873 K from Lenev and Novokhatskiy [40] and obtained $\Delta G^f_{MnCr_2O_4} = -52.6$ kJ. If one uses other values for $\Delta G^f_{MnAl_2O_4}$ reported in literature one may obtain e.g. $\Delta G^f_{MnCr_2O_4} = -51.5$ kJ [38], −54.4 kJ [41] and −35.6 kJ [42] at 1873 K and −50.7 kJ [38], −53.6 kJ [41] and −34.8 kJ [42] at 1773 K.

Jacob et al. [43] used the same technique as Tsai and Muan [39] and calculated the standard Gibbs energy changes at 1373 K for Eq. (9) using the activity data for the spinel phase obtained in their study and data for the corundum phase from a previous work [44] on the Al_2O_3–Cr_2O_3 system. Using $\Delta G^f_{MnAl_2O_4}$ from Barin [38]$\Delta G^f_{MnCr_2O_4} = -57.5 \pm 2.4$ kJ could be calculated.

Biggers [45] studied the ternary system CoO–MnO–Cr_2O_3 by approximately the same technique as Tsai and Muan [39] and found that $\Delta G^f_{MnCr_2O_4} = -59.0$ kJ at 1523 K.

Hasting and Corliss [46] investigated the magnetic structure and properties of $MnCr_2O_4$ by means of neutron diffraction. They reported that $MnCr_2O_4$ is a normal spinel at room-temperature with less than 1% Mn^{+2} ions present on octahedral sites. No experiments to study the temperature dependence of the cation distribution in $MnCr_2O_4$ have been reported.

Speidel and Muan [47] studied the Cr–Mn–O system in air in the temperature range 873–2253 K. Their reported solubility of Cr in Mn_2O_3 and Mn in Cr_2O_3 are considerable higher than the ones reported by Golikov et al. [48] and Pollert et al. [49,50]. Golikov et al. [48] made X-ray analysis for the Cr–Mn–O system in air in the temperature range 973–1673 K. They suggest that the temperature for the three-phase equilibrium β-spinel + Mn_2O_3 + Cr_2O_3 equilibrated in air is 973 K, but they did not perform any experiments at lower temperatures. Pollert et al. [49] performed annealing experiments in order to determine the α/β-spinel phase boundary in the temperature range from 1215 to 1395 K. They also reported a very high solubility limit of Cr in Mn_2O_3, which corresponds to an oxygen partial pressure ≫0.21 atm. Later, Pollert et al. [50] reinvestigated the phase equilibria between Mn_2O_3 and β-spinel and found a lower solubility, which agrees with that found by Geller and Espinosa [51], who measured the maximum solubility of Cr in Mn_2O_3 to 13 mol.%. Pollert et al. [50] also investigated the Cr_2O_3/β-spinel equilibria and the α/β-spinel equilibria in the temperature range 1100–1620 K. The experimentally determined three-phase equilibria equilibrated in air from these four authors [47–50] are summarized in Table 1.

Naoumidis et al. [52] investigated the Cr–Mn–O system at 1273 K both in air and in an Ar–4 vol.% H_2 atmosphere ($p_{O_2} \approx 10^{-21}$ bar).

Garbers-Craig and Dippenaar [53] studied the Cr–Mn–O system in a CO/CO_2=4.8 atmosphere in the temperature range 1673–2023 K.

Holba et al. [54] investigated the α/β-spinel transition temperature of $Mn_xCr_{3-x}O_4$ samples in the temperature range from 569 to 1445 K. At room-temperature, they found that samples with $1.0 \le x \le 1.76$ were cubic spinels and samples with $1.80 \le x \le 3.0$ corresponded to the tetragonal spinel.

The Mn-content in bcc for the three-phase equilibrium halite + β-spinel+bcc was measured by Ranganathan and Hajra [55] to be $x_{Mn} = 0.252$ at 1323 K.

Bobov et al. [56] investigated the two-phase equilibria β-spinel/halite at 1073, 1173 and 1273 K in an atmosphere with an oxygen partial pressure ranging from 10^{-13} to 10^{-1} Pa. They found that the lattice parameters of β-spinel changed with the oxygen partial pressure, but made a mistake when they used their results. They assumed that the composition of the spinel varied linearly with the H_2O/H_2 ratio which is not true. Later, Naoumidis et al. [52] measured the relationship between the lattice parameter and the composition at 1273 K. In the present study, the composition of β-spinel was recalculated, based on the data from Naoumidis et al. [52].

Table 1
Three-phase equilibria in the Cr–Mn–O system in air.

Equilibrium	Temperature (K)	Reference
β-Spinel + Mn_2O_3 + Cr_2O_3	973	Golikov et al. [48]
	<873	Speidel and Muan [47]
	813	This work
β-Spinel + α-spinel + Mn_2O_3	1183 ± 10	Golikov et al. [48]
	1183 ± 5	Speidel and Muan [47]
	1235	Pollert et al. [49]
	<1180	Pollert et al. [50]
	1177	This work
β-Spinel + Cr_2O_3 + liquid	2243 ± 20	Speidel and Muan [47]
	2465	This work

Tanahashi et al. [57] determined the phase equilibria for the Cr–Mn–O system at 1873 K as a function of P_{O2} ($2 \times 10^{-6} - 2 \times 10^{2}$ Pa). They found an increasing solubility of Cr in cubic $Mn_xCr_{3-x}O_4$ with decreasing oxygen partial pressure and an increasing solubility of Mn in cubic $Mn_xCr_{3-x}O_4$ with increasing oxygen partial pressure.

4. Optimisation and results

The optimisation of the parameters was performed using the PARROT module of the Thermo-Calc software package [10]. The values for the model parameters assessed in this work are listed in Table 2 . Data for the pure elements were taken from Dinsdale [58].

Using the scattered experimental data for the Gibbs energy of formation of $MnCr_2O_4$ from MnO and Cr_2O_3 ($\Delta G^f_{MnCr_2O_4} = \Delta H^f_{MnCr_2O_4} + \Delta S^f_{MnCr_2O_4} T$), it is difficult to evaluate any temperature dependence, and $\Delta S^f_{MnCr_2O_4} = 0$ was therefore assumed. In the optimisation, low weight was given to these data and higher weight to the phase diagram data. The enthalpy of formation, $\Delta H^f_{MnCr_2O_4}$, is optimised to be −51.0 kJ/mol. The optimised Gibbs energy of formation of $MnCr_2O_4$ from MnO and Cr_2O_3 is shown in Fig. 2 together with the experimental data.

Since no detailed studies on the cation distribution is available, $\Delta G^{\beta}_{2C:2C} = 0$ was chosen, see Section 2.2. This choice will give an almost perfectly normal spinel for all temperatures. At 1273 K, the

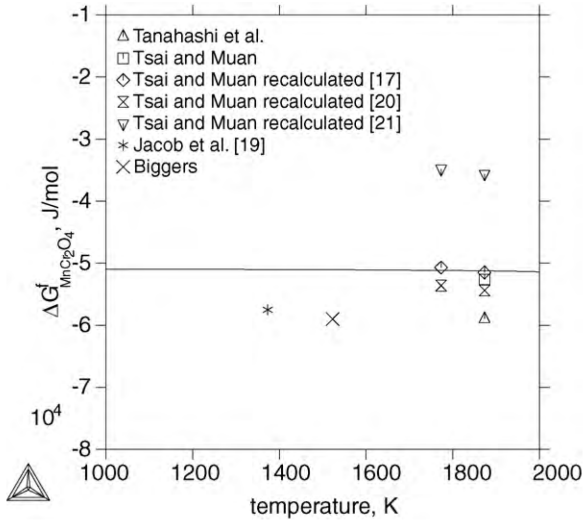

Fig. 2. Calculated and experimental [37,39,43,45] Gibbs energy of formation for $MnCr_2O_4$.

Table 2
Assessed parameters (in SI units; J, mole, K.)

The magnetic contribution to Gibbs energy is described by:
$G^{magn} = RT\ln(\beta+1)f(\tau),\ \tau = T/T_C$
For $\tau < 1$:
$f(\tau) = 1 - \frac{[(79\tau^{-1}/140p)+(474/497)((1/p)-1)((\tau^3/6)+(\tau^9/135)+(\tau^{15}/600))]}{A}$
and for $\tau > 1$:
$f(\tau) = \frac{-((\tau^{-5}/10)+(\tau^{-15}/315)+(\tau^{-25}/1500))}{A}$
where $A = (518/1125) + (11,692/15,975)((1/p) - 1)$ and p depends on the structure.

Liquid $(\mathrm{Cr}^{+2}, \mathrm{Mn}^{+2})_P(\mathrm{O}^{-2}, \mathrm{Va}^{-Q}, \mathrm{CrO}_{1.5}, \mathrm{MnO}_{1.5})_Q$
$^{o}G_{\mathrm{Cr}^{+2}:\mathrm{O}^{-2}} - 2H^{\mathrm{SER}}_{\mathrm{Cr}} - 2H^{\mathrm{SER}}_{\mathrm{O}} = \mathrm{2GCR1O1\_L}$
$^{o}G_{\mathrm{Cr}^{+2}:\mathrm{Va}} - H^{\mathrm{SER}}_{\mathrm{Cr}} = \mathrm{GCR\_L}$
$^{o}G_{\mathrm{CrO}_{1.5}} - H^{\mathrm{SER}}_{\mathrm{Mn}} - 1.5H^{\mathrm{SER}}_{\mathrm{O}} = \mathrm{0.5GCR2O3\_L}$
$^{o}G_{\mathrm{Mn}^{+2}:\mathrm{O}^{-2}} - 2H^{\mathrm{SER}}_{\mathrm{Mn}} - 2H^{\mathrm{SER}}_{\mathrm{O}} = \mathrm{2GMN1O1\_L}$
$^{o}G_{\mathrm{Mn}^{+2}:\mathrm{Va}} - H^{\mathrm{SER}}_{\mathrm{Mn}} = \mathrm{GMN\_L}$
$^{o}G_{\mathrm{MnO}_{1.5}} - H^{\mathrm{SER}}_{\mathrm{Mn}} - 1.5H^{\mathrm{SER}}_{\mathrm{O}} = \mathrm{0.5GMN2O3\_L}$
$^{0}L_{\mathrm{Cr}^{+2}:\mathrm{O}^{-2},\mathrm{Va}} = 208,000 - 53T$
$^{1}L_{\mathrm{Cr}^{+2}:\mathrm{O}^{-2},\mathrm{Va}} = -21,000$
$^{0}L_{\mathrm{Mn}^{+2}:\mathrm{O}^{-2},\mathrm{Va}} = 129,519$
$^{1}L_{\mathrm{Mn}^{+2}:\mathrm{O}^{-2},\mathrm{Va}} = -45,459$
$^{0}L_{\mathrm{Cr}^{+2}:\mathrm{O}^{-2},\mathrm{CrO}_{1.5}} = 47,000$
$^{0}L_{\mathrm{Mn}^{+2}:\mathrm{O}^{-2},\mathrm{MnO}_{1.5}} = -33,859$
$^{0}L_{\mathrm{Cr}^{+2}:\mathrm{Va},\mathrm{CrO}_{1.5}} = 110,000$
$^{0}L_{\mathrm{Cr}^{+2}:\mathrm{Va}Va,\mathrm{MnO}_{1.5}} = 110,000$
$^{0}L_{\mathrm{Mn}^{+2}:\mathrm{Va},\mathrm{CrO}_{1.5}} = 110,000$
$^{0}L_{\mathrm{Mn}^{+2}:\mathrm{Va},\mathrm{MnO}_{1.5}} = 110,000$
$^{0}L_{\mathrm{Cr}^{+2},\mathrm{Mn}^{+2}:\mathrm{Va}} = -15,009 + 13.6587T$
$^{1}L_{\mathrm{Cr}^{+2},\mathrm{Mn}^{+2}:\mathrm{Va}} = 504 + 0.9479T$

Halite: $(\mathrm{Cr}^{+3}, \mathrm{Mn}^{2+}, \mathrm{Mn}^{3+}, \mathrm{Va})_1(\mathrm{O}^{2-})_1$
$^{o}G_{\mathrm{Cr}^{+3}:\mathrm{O}^{-2}} - H^{\mathrm{SER}}_{\mathrm{Cr}} - H^{\mathrm{SER}}_{\mathrm{O}} = \mathrm{CWUSTITE}$
$^{o}G_{\mathrm{Mn}^{+2}:\mathrm{O}^{-2}} - H^{\mathrm{SER}}_{\mathrm{Mn}} - H^{\mathrm{SER}}_{\mathrm{O}} = \mathrm{GMN1O1}$
$^{o}G_{\mathrm{Mn}^{+3}:\mathrm{O}^{-2}} - H^{\mathrm{SER}}_{\mathrm{Mn}} - H^{\mathrm{SER}}_{\mathrm{O}} = \mathrm{GMN1O1} - 21,884 - 22.185T$
$^{o}G_{\mathrm{Va}:\mathrm{O}^{-2}} - H^{\mathrm{SER}}_{\mathrm{O}} = 0$
$^{0}L_{\mathrm{Mn}^{+2},\mathrm{Mn}^{+3}:\mathrm{O}^{-2}} = -42,105$
$^{1}L_{\mathrm{Mn}^{+2},\mathrm{Mn}^{+3}:\mathrm{O}^{-2}} = 46,513$
$^{0}L_{\mathrm{Cr}^{+3},\mathrm{Mn}^{+2}:\mathrm{O}^{-2}} = 23,000$ [a]

Pyrolusite (MnO_2): $(\mathrm{Mn}^{+4})_1(\mathrm{O}^{-2})_2$
$^{o}G_{\mathrm{Mn}^{+4}:\mathrm{O}^{-2}} - H^{\mathrm{SER}}_{\mathrm{Mn}} - 2H^{\mathrm{SER}}_{\mathrm{O}} = -545,091 + 395.379T - 65.277T\ln T - 0.007803T^2 + 664,955/T$

Bixbyite: $(\mathrm{Cr}^{+3}, \mathrm{Mn}^{+3})_2(\mathrm{O}^{-2})_3$
$^{o}G_{\mathrm{Cr}^{+3}:\mathrm{O}^{-2}} - 2H^{\mathrm{SER}}_{\mathrm{Cr}} - 3H^{\mathrm{SER}}_{\mathrm{O}} = \mathrm{GCR2O3} + 39,000 - 13T$ [a]
$^{o}G_{\mathrm{Mn}^{+3}:\mathrm{O}^{-2}} - 2H^{\mathrm{SER}}_{\mathrm{Mn}} - 3H^{\mathrm{SER}}_{\mathrm{O}} = \mathrm{GMN2O3}$
$^{0}L_{\mathrm{Cr}^{+3},\mathrm{Mn}^{+3}:\mathrm{O}^{-2}} = -25,000$ [a]

Corundum: $(\mathrm{Cr}^{+2}, \mathrm{Cr}^{+3}, \mathrm{Mn}^{+3})_2(\mathrm{Cr}^{+3}, \mathrm{Va})_1(\mathrm{O}^{-2})_3$
$^{o}G_{\mathrm{Cr}^{+2}:\mathrm{Va}:\mathrm{O}^{-2}} - 2H^{\mathrm{SER}}_{\mathrm{Cr}} - 3H^{\mathrm{SER}}_{\mathrm{O}} = \mathrm{GCR2O3}$
$^{o}G_{\mathrm{Cr}^{+3}:\mathrm{Va}:\mathrm{O}^{-2}} - 2H^{\mathrm{SER}}_{\mathrm{Cr}} - 3H^{\mathrm{SER}}_{\mathrm{O}} = \mathrm{GCR2O3}$
$^{o}G_{\mathrm{Cr}^{+2}:\mathrm{Cr}^{+3}:\mathrm{O}^{-2}} - 3H^{\mathrm{SER}}_{\mathrm{Cr}} - 3H^{\mathrm{SER}}_{\mathrm{O}} = \mathrm{GCR2O3} + 665,910$
$^{o}G_{\mathrm{Cr}^{+3}:\mathrm{Cr}^{+3}:\mathrm{O}^{-2}} - 3H^{\mathrm{SER}}_{\mathrm{Cr}} - 3H^{\mathrm{SER}}_{\mathrm{O}} = \mathrm{GCR2O3} - 232,227.2 + 241.3793T$
$^{o}G_{\mathrm{Mn}^{+3}:\mathrm{Va}:\mathrm{O}^{-2}} - 2H^{\mathrm{SER}}_{\mathrm{Mn}} - 3H^{\mathrm{SER}}_{\mathrm{O}} = \mathrm{GMN2O3} + 25,500 - 3.7T$
$^{o}G_{\mathrm{Mn}^{+3}:\mathrm{Cr}^{+3}:\mathrm{O}^{-2}} - 2H^{\mathrm{SER}}_{\mathrm{Mn}} - H^{\mathrm{SER}}_{\mathrm{Cr}} - 3H^{\mathrm{SER}}_{\mathrm{O}} = \mathrm{GMN2O3} + 300,000$ [a]
$^{0}L_{\mathrm{Cr}^{+3},\mathrm{Mn}^{+3}:\mathrm{Va}:\mathrm{O}^{-2}} = 15,000$ [a]
Magnetic properties ($p = 0.28$):
for compounds containing only Cr cations $T_C = -918$ and $\beta = -5.814$
for compounds containing Mn cations $T_C = 0$ and $\beta = 0$

β-Spinel: $(\mathrm{Cr}^{+2}, \mathrm{Cr}^{+3}, \mathrm{Mn}^{+2})_1(\mathrm{Cr}^{+3}, \mathrm{Mn}^{+2}, \mathrm{Mn}^{+3}, \mathrm{Mn}^{+4}, \mathrm{Va})_2(\mathrm{Cr}^{+2}, \mathrm{Mn}^{+2}, \mathrm{Va})_2(\mathrm{O}^{-2})_4$
$^{o}G_{\mathrm{Cr}^{+2}:\mathrm{Cr}^{+3}:\mathrm{Va}:\mathrm{O}^{-2}} - 3H^{\mathrm{SER}}_{\mathrm{Cr}} - 4H^{\mathrm{SER}}_{\mathrm{O}} = \mathrm{10.5GFCB} - \mathrm{3.5GFFB} - \mathrm{0.5JFF} + \mathrm{JFC} + \mathrm{GCCB}$
$^{o}G_{\mathrm{Cr}^{+2}:\mathrm{Va}:\mathrm{Va}:\mathrm{O}^{-2}} - H^{\mathrm{SER}}_{\mathrm{Cr}} - 4H^{\mathrm{SER}}_{\mathrm{O}} = \mathrm{3.5GFCB} + \mathrm{1.5GFFB} - \mathrm{0.5JFF} + \mathrm{C} + \mathrm{JFC} + \mathrm{GCCB}$
$^{o}G_{\mathrm{Cr}^{+3}:\mathrm{Cr}^{+3}:\mathrm{Va}:\mathrm{O}^{-2}} - 3H^{\mathrm{SER}}_{\mathrm{Cr}} - 4H^{\mathrm{SER}}_{\mathrm{O}} = \mathrm{10.5GFCB} - \mathrm{3.5GFFB} - \mathrm{0.5JFF} + \mathrm{JFC}$
$^{o}G_{\mathrm{Cr}^{+3}:\mathrm{Va}:\mathrm{Va}:\mathrm{O}^{-2}} - H^{\mathrm{SER}}_{\mathrm{Cr}} - 4H^{\mathrm{SER}}_{\mathrm{O}} = \mathrm{3.5GFCB} + \mathrm{1.5GFFB} - \mathrm{0.5JFF} + \mathrm{C} + \mathrm{JFC}$
$^{o}G_{\mathrm{Mn}^{+2}:\mathrm{Mn}^{+2}:\mathrm{Va}:\mathrm{O}^{-2}} - 3H^{\mathrm{SER}}_{\mathrm{Mn}} - 4H^{\mathrm{SER}}_{\mathrm{O}} = \mathrm{GM2M2B}$
$^{o}G_{\mathrm{Mn}^{+2}:\mathrm{Mn}^{+3}:\mathrm{Va}:\mathrm{O}^{-2}} - 3H^{\mathrm{SER}}_{\mathrm{Mn}} - 4H^{\mathrm{SER}}_{\mathrm{O}} = \mathrm{7GMMB}$
$^{o}G_{\mathrm{Mn}^{+2}:\mathrm{Mn}^{+4}:\mathrm{Va}:\mathrm{O}^{-2}} - 3H^{\mathrm{SER}}_{\mathrm{Mn}} - 4H^{\mathrm{SER}}_{\mathrm{O}} = \mathrm{14GMMB} + \mathrm{JMMB} - \mathrm{GM2M2B}$
$^{o}G_{\mathrm{Mn}^{+2}:\mathrm{Va}:\mathrm{Va}:\mathrm{O}^{-2}} - H^{\mathrm{SER}}_{\mathrm{Mn}} - 4H^{\mathrm{SER}}_{O} = \mathrm{8GGMN2O3B} - \mathrm{56GMMB} - \mathrm{3JMMB} + \mathrm{3GM2M2B} + 2RT(6\ln 6 - 3\ln 3 - 2\ln 2)$
$^{o}G_{\mathrm{Cr}^{+2}:\mathrm{Mn}^{+2}:\mathrm{Va}:\mathrm{O}^{-2}} - H^{\mathrm{SER}}_{\mathrm{Cr}} - 2H^{\mathrm{SER}}_{\mathrm{Mn}} - 4H^{\mathrm{SER}}_{\mathrm{O}} = \mathrm{GM2M2B} - \mathrm{7GMCB} + \mathrm{10.5GFCB} - \mathrm{3.5GFFB} - \mathrm{0.5JFF} + \mathrm{JFC} + \mathrm{GCCB}$
$^{o}G_{\mathrm{Cr}^{+2}:\mathrm{Mn}^{+3}:\mathrm{Va}:\mathrm{O}^{-2}} - H^{\mathrm{SER}}_{\mathrm{Cr}} - 2H^{\mathrm{SER}}_{\mathrm{Mn}} - 4H^{\mathrm{SER}}_{\mathrm{O}} = \mathrm{7GMMB} - \mathrm{7GMCB} + \mathrm{10.5GFCB} - \mathrm{3.5GFFB} - \mathrm{0.5JFF} + \mathrm{JFC} + \mathrm{GCCB}$
$^{o}G_{\mathrm{Cr}^{+2}:\mathrm{Mn}^{+4}:\mathrm{Va}:\mathrm{O}^{-2}} - H^{\mathrm{SER}}_{\mathrm{Cr}} - 2H^{\mathrm{SER}}_{\mathrm{Mn}} - 4H^{\mathrm{SER}}_{\mathrm{O}} = \mathrm{14GMMB} - \mathrm{GM2M2B} + \mathrm{JMMB} - \mathrm{7GMCB} + \mathrm{10.5GFCB} - \mathrm{3.5GFFB} - \mathrm{0.5JFF} + \mathrm{JFC} + \mathrm{GCCB}$
$^{o}G_{\mathrm{Cr}^{+3}:\mathrm{Mn}^{+2}:\mathrm{Va}:\mathrm{O}^{-2}} - H^{\mathrm{SER}}_{\mathrm{Cr}} - 2H^{\mathrm{SER}}_{\mathrm{Mn}} - 4H^{\mathrm{SER}}_{\mathrm{O}} = \mathrm{GM2M2B} - \mathrm{7GMCB} + \mathrm{10.5GFCB} - \mathrm{3.5GFFB} - \mathrm{0.5JFF} + \mathrm{JFC}$
$^{o}G_{\mathrm{Cr}^{+3}:\mathrm{Mn}^{+3}:\mathrm{Va}:\mathrm{O}^{-2}} - H^{\mathrm{SER}}_{\mathrm{Cr}} - 2H^{\mathrm{SER}}_{\mathrm{Mn}} - 4H^{\mathrm{SER}}_{\mathrm{O}} = \mathrm{7GMMB} - \mathrm{7GMCB} + \mathrm{10.5GFCB} - \mathrm{3.5GFFB} - \mathrm{0.5JFF} + \mathrm{JFC}$
$^{o}G_{\mathrm{Cr}^{+3}:\mathrm{Mn}^{+4}:\mathrm{Va}:\mathrm{O}^{-2}} - H^{\mathrm{SER}}_{\mathrm{Cr}} - 2H^{\mathrm{SER}}_{\mathrm{Mn}} - 4H^{\mathrm{SER}}_{\mathrm{O}} = \mathrm{14GMMB} - \mathrm{GM2M2B} + \mathrm{JMMB} - \mathrm{7GMCB} + \mathrm{10.5GFCB} - \mathrm{3.5GFFB} - \mathrm{0.5JFF} + \mathrm{JFC}$
$^{o}G_{\mathrm{Mn}^{+2}:\mathrm{Cr}^{+3}:\mathrm{Va}:\mathrm{O}^{-2}} - 2H^{\mathrm{SER}}_{\mathrm{Cr}} - H^{\mathrm{SER}}_{\mathrm{Mn}} - 4H^{\mathrm{SER}}_{\mathrm{O}} = \mathrm{7GMCB}$
$^{o}G_{*:*:\mathrm{Cr}^{+2}:\mathrm{O}^{-2}} = {}^{o}G_{*:*:\mathrm{Va}:\mathrm{O}^{-2}} + \mathrm{2GFFB} + \mathrm{D} - \mathrm{JFF}$
$^{o}G_{*:*:\mathrm{Mn}^{+2}:\mathrm{O}^{-2}} = {}^{o}G_{*:*:\mathrm{Va}:\mathrm{O}^{-2}} + \mathrm{8GGMN1O1B} - \mathrm{2GM2M2B} + 4RT\ln 2$
$^{o}G_{\mathrm{Mn}^{+2}:\mathrm{Cr}^{+3}:\mathrm{Mn}^{+2}:\mathrm{O}^{-2}} = {}^{o}G_{\mathrm{Mn}^{+2}:\mathrm{Cr}^{+3}:\mathrm{Va}:\mathrm{O}^{-2}} + \mathrm{8GGMN1O1B} - \mathrm{2GM2M2B} + 4RT\ln 2 + 145,000$ [a]
Magnetic properties ($p = 0.28$):
for compounds containing only Cr cations $T_C = 100$ and $\beta = 0.9$
for compounds containing only Mn cations $T_C = 43.15$ and $\beta = 0$

Table 2 (*Continued*)

α-Spinel: $(\mathrm{Cr^{+2}, Cr^{+3}, Mn^{+2}, Mn^{+3}})_1(\mathrm{Cr^{+3}, Mn^{+2}, Mn^{+3}, Va})_2(\mathrm{Cr^{+2}, Mn^{+2}, Va})_2(\mathrm{O^{-2}})_4$

${}^{o}G_{\mathrm{Cr^{+2}:Cr^{+3}:Va:O^{-2}}} - 3H_{\mathrm{Cr}}^{\mathrm{SER}} - 4H_{\mathrm{O}}^{\mathrm{SER}} = 10.5\mathrm{GFCA} - 3.5\mathrm{GFFA} - 0.5\mathrm{JFF} + \mathrm{JFC} + \mathrm{GCCA}$

${}^{o}G_{\mathrm{Cr^{+2}:Va:Va:O^{-2}}} - H_{\mathrm{Cr}}^{\mathrm{SER}} - 4H_{\mathrm{O}}^{\mathrm{SER}} = 3.5\mathrm{GFCA} + 1.5\mathrm{GFFA} - 0.5\mathrm{JFF} + \mathrm{C} + \mathrm{JFC} + \mathrm{GCCA}$

${}^{o}G_{\mathrm{Cr^{+3}:Cr^{+3}:Va:O^{-2}}} - 3H_{\mathrm{Cr}}^{\mathrm{SER}} - 4H_{\mathrm{O}}^{\mathrm{SER}} = 10.5\mathrm{GFCA} - 3.5\mathrm{GFFA} - 0.5\mathrm{JFF} + \mathrm{JFC}$

${}^{o}G_{\mathrm{Cr^{+3}:Va:Va:O^{-2}}} - H_{\mathrm{Cr}}^{\mathrm{SER}} - 4H_{\mathrm{O}}^{\mathrm{SER}} = 3.5\mathrm{GFCA} + 1.5\mathrm{GFFA} - 0.5\mathrm{JFF} + \mathrm{C} + \mathrm{JFC}$

${}^{o}G_{\mathrm{Mn^{+2}:Mn^{+2}:Va:O^{-2}}} - 3H_{\mathrm{Mn}}^{\mathrm{SER}} - 4H_{\mathrm{O}}^{\mathrm{SER}} = 21\mathrm{GMMA} + 2\mathrm{JMMA} - 2\mathrm{GM3M3A}$

${}^{o}G_{\mathrm{Mn^{+3}:Mn^{+2}:Va:O^{-2}}} - 3H_{\mathrm{Mn}}^{\mathrm{SER}} - 4H_{\mathrm{O}}^{\mathrm{SER}} = 14\mathrm{GMMA} + 2\mathrm{JMMA} - \mathrm{GM3M3A}$

${}^{o}G_{\mathrm{Mn^{+2}:Mn^{+3}:Va:O^{-2}}} - 3H_{\mathrm{Mn}}^{\mathrm{SER}} - 4H_{\mathrm{O}}^{\mathrm{SER}} = 7\mathrm{GMMA}$

${}^{o}G_{\mathrm{Mn^{+3}:Mn^{+3}:Va:O^{-2}}} - 3H_{\mathrm{Mn}}^{\mathrm{SER}} - 4H_{\mathrm{O}}^{\mathrm{SER}} = \mathrm{GM3M3A}$

${}^{o}G_{\mathrm{Mn^{+2}:Va:Va:O^{-2}}} - H_{\mathrm{Mn}}^{\mathrm{SER}} - 4H_{\mathrm{O}}^{\mathrm{SER}} = 8\mathrm{GGMN2O3A} - 6\mathrm{GM3M3A} + 7\mathrm{GMMA} + 2RT(6\ln 6 - 5\ln 5)$

${}^{o}G_{\mathrm{Mn^{+3}:Va:Va:O^{-2}}} - H_{\mathrm{Mn}}^{\mathrm{SER}} - 4H_{\mathrm{O}}^{\mathrm{SER}} = 8\mathrm{GGMN2O3A} - 5\mathrm{GM3M3A} + 2RT(6\ln 6 - 5\ln 5)$

${}^{o}G_{\mathrm{Cr^{+2}:Mn^{+2}:Va:O^{-2}}} - H_{\mathrm{Cr}}^{\mathrm{SER}} - 2H_{\mathrm{Mn}}^{\mathrm{SER}} - 4H_{\mathrm{O}}^{\mathrm{SER}} = 10.5\mathrm{GFCA} - 3.5\mathrm{GFFA} - 0.5\mathrm{JFF} + \mathrm{JFC} + \mathrm{GCCA} + 21\mathrm{GMMA} + 2\mathrm{JMMA} - 2\mathrm{GM3M3A} - 7\mathrm{GMCA}$

${}^{o}G_{\mathrm{Cr^{+2}:Mn^{+3}:Va:O^{-2}}} - H_{\mathrm{Cr}}^{\mathrm{SER}} - 2H_{\mathrm{Mn}}^{\mathrm{SER}} - 4H_{\mathrm{O}}^{\mathrm{SER}} = 10.5\mathrm{GFCA} - 3.5\mathrm{GFFA} - 0.5\mathrm{JFF} + \mathrm{JFC} + \mathrm{GCCA} + 7\mathrm{GMMA} - 7\mathrm{GMCA}$

${}^{o}G_{\mathrm{Cr^{+3}:Mn^{+2}:Va:O^{-2}}} - H_{\mathrm{Cr}}^{\mathrm{SER}} - 2H_{\mathrm{Mn}}^{\mathrm{SER}} - 4H_{\mathrm{O}}^{\mathrm{SER}} = 10.5\mathrm{GFCA} - 3.5\mathrm{GFFA} - 0.5\mathrm{JFF} + \mathrm{JFC} + 21\mathrm{GMMA} + 2\mathrm{JMMA} - 2\mathrm{GM3M3A} - 7\mathrm{GMCA}$

${}^{o}G_{\mathrm{Cr^{+3}:Mn^{+3}:Va:O^{-2}}} - H_{\mathrm{Cr}}^{\mathrm{SER}} - 2H_{\mathrm{Mn}}^{\mathrm{SER}} - 4H_{\mathrm{O}}^{\mathrm{SER}} = 10.5\mathrm{GFCA} - 3.5\mathrm{GFFA} - 0.5\mathrm{JFF} + \mathrm{JFC} + 7\mathrm{GMMA} - 7\mathrm{GMCA}$

${}^{o}G_{\mathrm{Mn^{+2}:Cr^{+3}:Va:O^{-2}}} - 2H_{\mathrm{Cr}}^{\mathrm{SER}} - H_{\mathrm{Mn}}^{\mathrm{SER}} - 4H_{\mathrm{O}}^{\mathrm{SER}} = 7\mathrm{GMCA}$

${}^{o}G_{\mathrm{Mn^{+3}:Cr^{+3}:Va:O^{-2}}} - 2H_{\mathrm{Cr}}^{\mathrm{SER}} - H_{\mathrm{Mn}}^{\mathrm{SER}} - 4H_{\mathrm{O}}^{\mathrm{SER}} = 7\mathrm{GMCA} + \mathrm{GM3M3A} - 7\mathrm{GMMA}$

${}^{o}G_{*:*:\mathrm{Cr^{+2}:O^{-2}}} = {}^{o}G_{*:*:\mathrm{Va:O^{-2}}} + 2\mathrm{GFFA} + \mathrm{D} - \mathrm{JFF}$

${}^{o}G_{*:*:\mathrm{Mn^{+2}:O^{-2}}} = {}^{o}G_{*:*:\mathrm{Va:O^{-2}}} + 8\mathrm{GGMN1O1A} - 42\mathrm{GMMA} - 4\mathrm{JMMA} + 4\mathrm{GM3M3A} + 4RT\ln 2$

Magnetic properties ($p = 0.28$):

for compounds containing only Cr cations $T_C = 100$ and $\beta = 0.9$

for compounds containing only Mn cations $T_C = 43.15$ and $\beta = 0$

Functions

$\mathrm{GCR\_L}(298.15 < T < 2180) = \mathrm{GHSERCR} + 24, 339.955 - 11.420225T + 2.37615E - 21E - 21T^7$

$\mathrm{GCR\_L}(2180 < T < 6000) = -16, 459.984 + 335.616316T - 50T\ln T$

$\mathrm{GHSERCR}(298.15 < T < 2180) = -8856.94 + 157.48T - 26.908T\ln T + .00189435T^2 - 1.47721E - 06T^3 + 139, 250/T$

$\mathrm{GHSERCR}(2180 < T < 6000) = -34, 869.344 + 344.18T - 50T\ln T - 2.88526E + 32/T^9$

$\mathrm{GCR1O1\_L} = 0.5\mathrm{GCR2O3\_L} - 0.25 * GO2GAS + 189, 130 - 51T$

$\mathrm{GCR2O3}(298.15 < T < 1000) = -1, 177, 497.8 + 814.9138T - 132.046T\ln T + .005256015T^2 - 1.38885E - 06T^3 + 1, 501, 761/T$

$\mathrm{GCR2O3}(1000 < T < 2600) = -1, 166, 947.9 + 701.5624T - 115.5381T\ln T - .00620492T^2 + 1.00698E - 07T^3 + 239, 949/T$

$\mathrm{GCR2O3\_L} = -1, 047, 074 + 260.777T - 3.97112T\ln T + 2\mathrm{GCR\_L} + 1.5\mathrm{GO2GAS}$

$\mathrm{CWUSTITE}(298.15 < T < 1000) = -563, 748.9 + 407.4569T - 66.02315T\ln T + .002628T^2 - 6.944225E - 07T^3 + 750, 881/T$

$\mathrm{CWUSTITE}(1000 < T < 2600) = -558, 473.9 + 350.7812T - 57.76905T\ln T - .00310246T^2 + 5.034917E - 08T^3 + 119, 974.7/T$

$\mathrm{GMN\_L}(298.15 < T < 1519) = \mathrm{GHSERMN} + 17, 859.91 - 12.6208T - 4.41929E - 21T^7$

$\mathrm{GMN\_L}(1519 < T < 6000) = \mathrm{GHSERMN} + 18, 739.51 - 13.2288T - 1.656847E + 30/T^9$

$\mathrm{GMN1O1\_L} = \mathrm{GMN1O1} + 43, 947 - 20.628T$

$\mathrm{GMN1O1} = -402, 478 + 259.356T - 46.835T\ln T - .00385T^2 + 212, 922/T$

$\mathrm{GMN2O3\_L} = +2\mathrm{GMN1O1} + 0.5\mathrm{GO2GAS} - 64, 953 + 43.144T$

$\mathrm{GMN2O3} = -998, 618 + 588.619T - 101.956T\ln T - .018844T^2 + 589, 055/T$

$\mathrm{GHSERMN}(298.15 < T < 1519) = -8115.28 + 130.059T - 23.4582T\ln T - 0.00734768T^2 + 69, 827.1/T$

$\mathrm{GHSERMN}(1519 < T < 6000) = -28, 733.41 + 312.2648T - 48T\ln T + 1.656847E + 30/T^9$

$\mathrm{GO2GAS}(298.15 < T < 1000) = -6961.74451 - 51.0057202T - 22.2710136T\ln T - 0.0101977469T^2 + 1.32369208E - 06T^3 - 76, 729.7484/T$

$\mathrm{GO2GAS}(1000 < T < 3300) = -13, 137.5203 + 25.3200332T - 33.627603T\ln T - 0.00119159274T^2 + 1.35611111E - 08T^3 + 525, 809.556/T$

$\mathrm{GO2GAS}(3300 < T < 6000) = -27, 973.4908 + 62.5195726T - 37.9072074T\ln T - 8.50483772E - 04T^2 + 2.14409777E - 08T^3 + 8, 766, 421.4/T$

$\mathrm{GCCB} = 46, 028.95 + 38.73173T - 11.58574T\ln T + .006411774T^2$

$\mathrm{GCCA} = \mathrm{GCCB} + 1000$ [a]

$\mathrm{GFCB} = -214, 607.7 + 138.83T - 23.28714T\ln T - .001595929T^2 + 227, 729.3/T$

$\mathrm{GFCA} = \mathrm{GFCB} + 1000$ [a]

$\mathrm{JFC} = 156, 000 - 3.37T$

$\mathrm{GFFB} = -161, 731 + 144.873T - 24.9879T\ln T - 0.0011952256T^2 + 206, 520/T$

$\mathrm{GFFA} = \mathrm{GFFB} + 1000$

$\mathrm{JFF} = 46, 826 - 27.266T$

$\mathrm{C} = 120, 730 - 20.102T$

$\mathrm{D} = 402, 520 - 30.529T$

$\mathrm{GMCOB} = \mathrm{GMN1O1} + \mathrm{GCR2O3} - 51, 000$ [a]

$\mathrm{GMCOA} = 2300 + 20T$ [a]

$\mathrm{GMCB} = \mathrm{GMCOB}/7$ [a]

$\mathrm{GMCA} = \mathrm{GMCOA}/7 + \mathrm{GMCOB}/7$ [a]

$\mathrm{GMFB} = -181, 660 + 125.8T - 22.08T\ln T - 0.0016T^2 + 104, 000/T$

$\mathrm{GMFA} = \mathrm{GMFB} + 4900 - 1.9T$

$\mathrm{JMF} = 28, 000$

$\mathrm{GMN3O4A} = -1, 439, 700 + 892.2T - 154.748T\ln T - 0.017408T^2 + 986, 139/T$

$\mathrm{GMN3O4B} = 15, 270 + 7T$

$\mathrm{GMMB} = \mathrm{GMN3O4B}/7 + \mathrm{GMN3O4A}/7$

$\mathrm{GMMA} = \mathrm{GMN3O4A}/7$

$\mathrm{JMMB} = 26, 210 - 17.46T$

$\mathrm{JMMA} = 95, 000$

$\mathrm{GGMN1O1B} = \mathrm{GMN1O1} + 66, 200 - 13.795T$

$\mathrm{GGMN2O3B} = \mathrm{GMN2O3} + 228, 000 - 200.34T + 0.05T^2$

$\mathrm{GM2M2B} = 21\mathrm{GMFB} + 2\mathrm{JMF} - 14\mathrm{GFFB} + 2\mathrm{JFF}$

$\mathrm{GGMN1O1A} = \mathrm{GMN1O1} + 58, 500 - 11T$

$\mathrm{GGMN2O3A} = \mathrm{GMN2O3} + 240, 000 - 211.8T + 0.05T^2$

$\mathrm{GM3M3A} = 10.5\mathrm{GMMA} + \mathrm{JMMA} - 10.5\mathrm{GMFA} - \mathrm{JMF} + 7\mathrm{GFFA} - \mathrm{JFF}$

---

[a] Parameters assessed in this work. Parameters for the Mn–O system originate from Grundy et al. [13], with revision regarding the liquid and spinel phases from Kjellqvist and Selleby [3]. Parameters from the Cr–O system originate from Taylor and Dinsdale [26,36], with revision regarding the liquid and spinel phases from Kjellqvist et al. [1,14]. Parameters for the metallic phases and the gas phase could be found elsewhere [12,58].

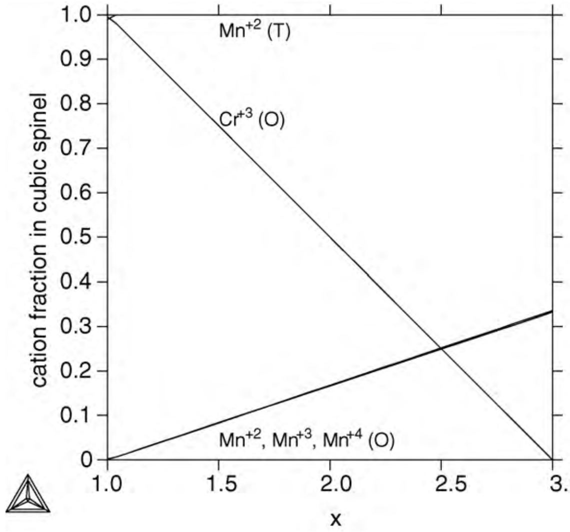

Fig. 3. Calculated cation distribution in $Mn_xCr_{3-x}O_4$ ($1 \leq x \leq 3$) at 1473 K. *T* and *O* represent tetrahedral and octahedral sites, respectively.

calculated fraction of Mn^{+2} ions on octahedral sites is 2×10^{-4}. The calculated cation distribution in $Mn_xCr_{3-x}O_4$ at 1473 K is shown in Fig. 3.

The experimental data for the Cr–Mn–O system in air are inconsistent. The measured single phase regions of α-spinel, Mn_2O_3 and Cr_2O_3 are much larger in the study by Speidel and Muan [47] than in other studies [48–50,52]. In the present work, the experimental data from Speidel and Muan [47] is not taken into consideration. Data from Pollert et al. [50] are used in the optimisation for the Mn_2O_3/β-spinel phase boundary. For the β-spinel/Cr_2O_3 boundary data from Pollert et al. [50], Tanahashi et al. [57], Naoumidis et al. [52] and Garbers-Craig and Dippenaar [53] are used. For the β-spinel/halite boundary, data from Bobov et al. [56], Tanahashi et al. [57] and Garbers-Craig and Dippenaar [53] are used.

For the tetragonal spinel, the only available data to determine the model parameters are the α/β-phase boundary and the transition temperature. Tetragonal $MnCr_2O_4$ is not a stable compound and the parameter ${}^{o}G^{\alpha}_{Mn^{+2}:Cr^{+3}}$ is optimised to reproduce the experimental data from Naoumidis et al. [52], Pollert et al. [49] and Holba et al. [54].

No good measurements for the Mn_2O_3 + β-spinel + Cr_2O_3 three-phase equilibrium in air is available. Speidel and Muan [47] reported that β-spinel should be stable below 873 K and Golikov et al. [48] claimed the temperature to be 973 K, but without doing any experiments at lower temperatures. The optimised temperature is 813 K. According to the present thermodynamic modelling, in order to be able to fit the temperature from Golikov et al. [48], the Gibbs energy of $MnCr_2O_4$ must be more than 8 kJ higher than the optimised value. If $MnCr_2O_4$ is assessed according to the measurements from Golikov et al., other experiments could not simultaneously be reproduced, e.g. the phase boundaries between β-spinel and Cr_2O_3 and between β-spinel + Mn_2O_3.

The only data for the liquid phase is the one from Speidel and Muan [47] who measured the three-phase equilibrium β-spinel+corundum + liquid to be at 2243 ± 20 K and $x_{Cr} = 0.63$. To be able to fit that temperature a rather large interaction parameter in the liquid phase is needed and another possibility is to instead use a temperature dependence for the Gibbs energy of formation of $MnCr_2O_4$. Povoden et al. [16] choose to assess a temperature dependence of $MnCr_2O_4$ in their Cr–Mn–O assessment and could then reproduce the temperature of the three-phase equilibrium β-spinel + corundum + liquid. This also led to a very low temperature for the three-phase equilibrium β-spinel + corundum + MnO_2. It is difficult to justify any of these approaches based on the insufficient experimental data available. Additional measurements on both these two three-phase equilibria would be desirable to obtain a more satisfactory description of this system. No ternary interaction parameters are used in the Cr–Mn–O liquid.

The calculated phase diagram in air, together with experimental data is shown in Fig. 4. Figs. 5 and 6 show the calculated composition-oxygen partial pressure phase diagram at 1273 and 1873 K with experimental data. The calculated phase diagram in an atmosphere with a CO:CO_2 volume ratio of 4.8, yielding oxygen partial pressures in the range $10^{-10} - 10^{-7}$, is shown in Fig. 7 together with the experimental data from Garbers-Craig and Dippenaar [53].

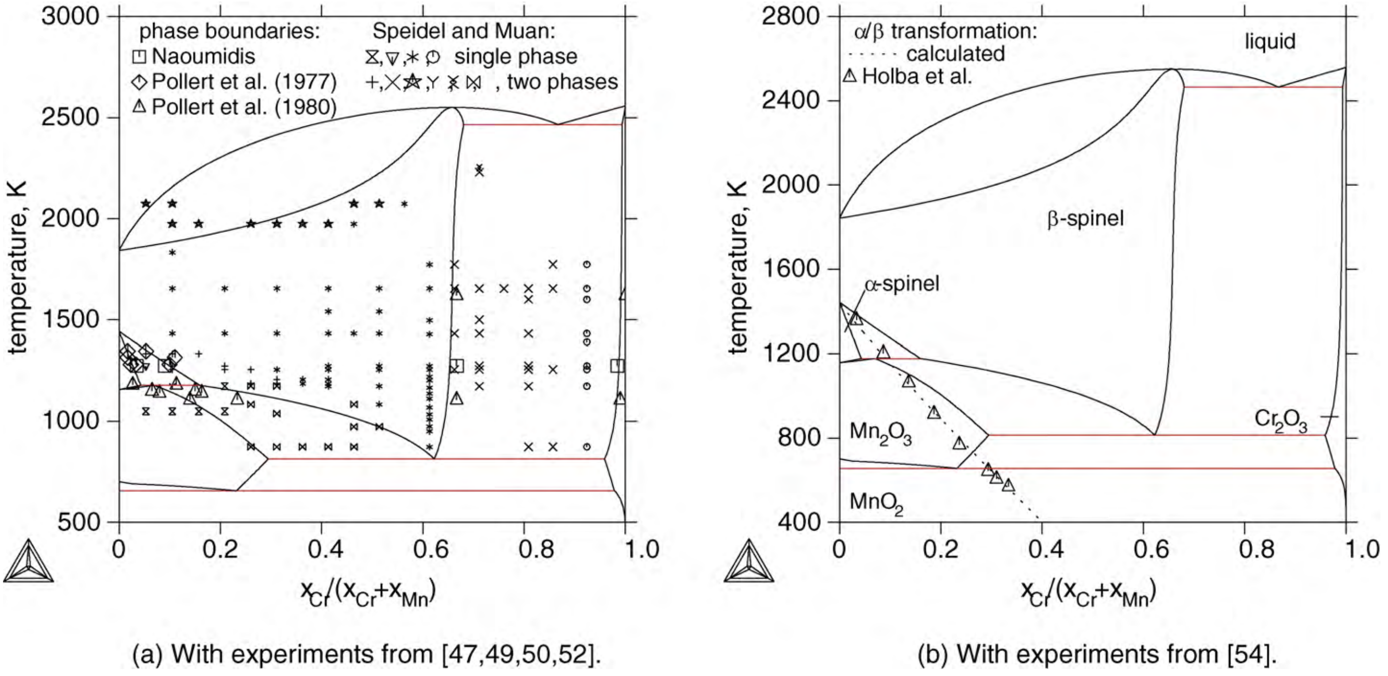

(a) With experiments from [47,49,50,52].

(b) With experiments from [54].

Fig. 4. Calculated phase diagram of Cr–Mn–O for a fixed pressure of 0.21 bar (air) with experimental data.

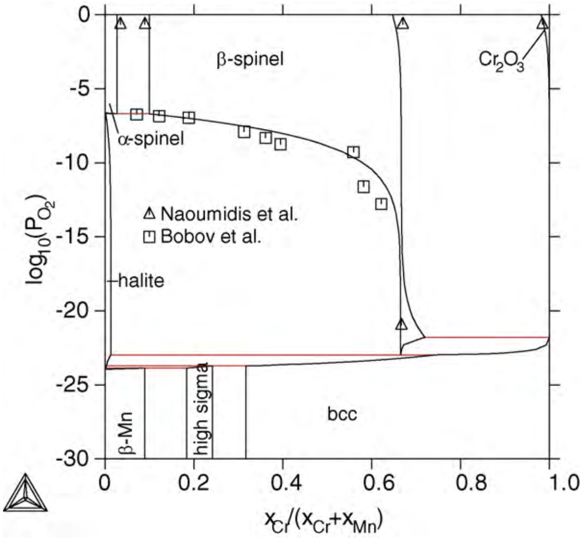

Fig. 5. Calculated and experimental [52,56] phase diagram at 1273 K.

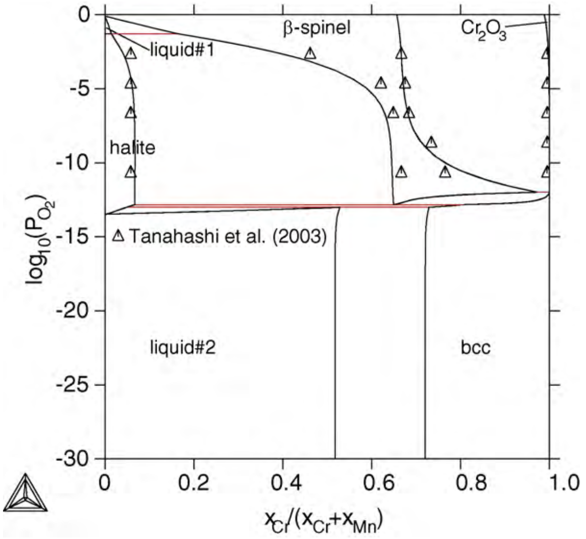

Fig. 6. Calculated and experimental [57] phase diagram at 1873 K.

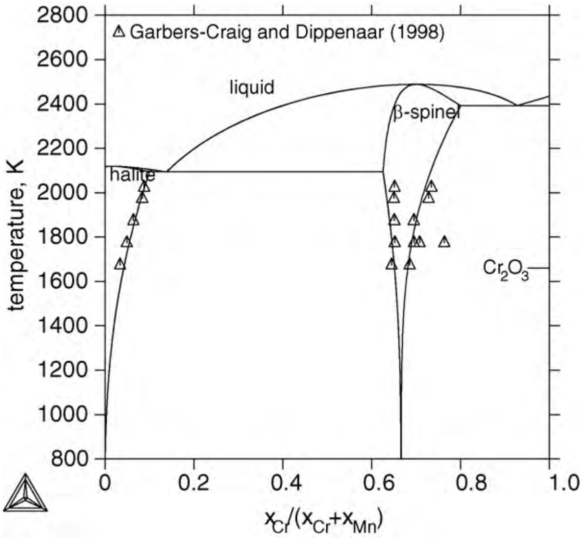

Fig. 7. Calculated and experimental [53] phase diagram of Cr–Mn–O in an atmosphere with CO/CO_2=4.8.

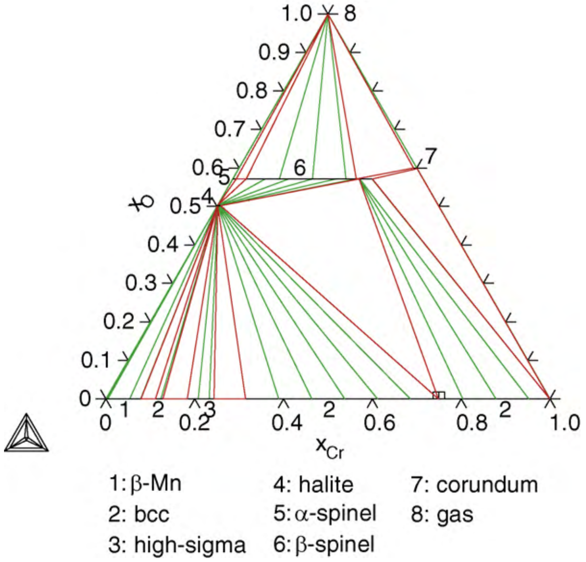

Fig. 8. Isothermal section of the Cr–Mn–O system at 1323 K, including the experimental point from Ranganathan and Hajra [55] on the three-phase equilibrium halite + β-spinel + bcc.

The calculated mole-fraction of Mn in bcc at the three-phase equilibrium halite + β-spinel+bcc at 1323 K is 0.252, in excellent agreement with the measured value reported by Ranganathan and Hajra [55]. An isothermal section of the ternary Cr-Mn-O system at 1323 K is shown in Fig. 8.

5. Conclusions

The present assessment gives a good description of the available experimental information in the ternary Cr–Mn–O system. A complete list of all parameters is found in Table 2. The Gibbs energy function of $MnCr_2O_4$ was evaluated based only on Gibbs energy of formation and phase diagram data. The description of the spinel phases in the Cr–Mn–O system is consistent with the description of the Fe–Cr–Ni–O [1], Fe–Mn–O [3] and Mn–Ni–O [4] spinel from earlier and ongoing work, and we are now able to do thermodynamic calculations in the five-component Fe–Cr–Mn–Ni–O system. The models in this work are compatible with the models used in a parallel work on the Al_2O_3–CaO–Fe–O–MgO–SiO_2 system [8,9].

Acknowledgements

This work was financially supported by the Swedish Steel Producers Association. The work has been performed within the framework of the Matop and CCT projects, both supported by the Swedish Foundation for Strategic Research (SSF) and industry.

References

[1] L. Kjellqvist, M. Selleby, B. Sundman, Calphad 32 (2008) 577–592.
[2] L. Kjellqvist, M. Selleby, Calphad 33 (2009) 393–397.
[3] L. Kjellqvist, M. Selleby, J. Phase Equilib. Diffus. 31 (2010) 113–134.
[4] L. Kjellqvist, M. Selleby, Int. J. Mat. Res. (formely Z. Metallkd.) (submitted for publication).
[5] J.-J. Choi, J. Ryu, B.-D. Hahn, W.-H. Yoon, B.-K. Lee, J.-H. Choi, D.-S. Park, J. Alloys Compd. 492 (2010) 488–495.
[6] Z.G. Yang, Int. Mater. Rev. 53 (2008) 39–54.
[7] J.W. Fergus, Mater. Sci. Eng. A 397 (2005) 271–283.
[8] H. Mao, M. Hillert, M. Selleby, B. Sundman, J. Am. Ceram. Soc. 89 (2006) 298–308.
[9] H. Mao, O. Fabrichnaya, M. Selleby, B. Sundman, J. Mater. Res. 20 (2005) 975–986.
[10] J.-O. Andersson, T. Helander, L. Hglund, P. Shi, B. Sundman, Calphad 26 (2002) 273–312.
[11] S. Hallstrm, L. Hglund, J. gren, The 6th European Stainless Steel Conference, Science and Market, Helsinki, Finland, June 10–13, 2008.

[12] B.-J. Lee, Metall. Trans. A 24A (1993) 1919–1933.
[13] A.N. Grundy, B. Hallstedt, L.J. Gauckler, J. Phase Equilib. 24 (2003) 21–39.
[14] L. Kjellqvist, M. Selleby (in preparation).
[15] I.-H. Jung, Solid State Ionics 177 (2006) 765–777.
[16] E. Povoden, A.N. Grundy, L.J. Gauckler, J. Phase Equilib. Diffus. 27 (2006) 353–362.
[17] S.A. Decterov, Y.-B. Kang, I.-H. Jung, J. Phase Equilib. Diffus. 30 (2009) 443–461.
[18] A.D. Pelton, M. Blander, Metall. Trans. B 17 (1986) 805–815.
[19] A.D. Pelton, S.A. Decterov, G. Eriksson, C. Robelin, Y. Dessureault, Metall. Mater. Trans. B 31 (2000) 651–659.
[20] A.D. Pelton, P. Chartrand, Metall. Mater. Trans. A 32 (2001) 1355–1360.
[21] M. Hillert, B. Jansson, B. Sundman, J. Ågren, Metall. Trans. A 16A (1985) 261–266.
[22] B. Sundman, Calphad 15 (1991) 109–119.
[23] B. Sundman, J. Phase Equilib. 12 (1991) 127–149.
[24] M. Selleby, B. Sundman, Calphad 20 (1996) 381–392.
[25] H. Mao, M. Selleby, B. Sundman, Calphad 28 (2004) 307–312.
[26] J.R. Taylor, A.T. Dinsdale, Z. Metallkd. 81 (1990) 354–366.
[27] M. Hillert, J. Alloys Compd. 320 (2001) 161–176.
[28] N. Saunders, A.P. Miodownik, Calphad (Calculation of Phase Diagrams): A Comprehensive Guide, 1998.
[29] H. Lukas, S.G. Fries, B. Sundman, Computational Thermodynamics: The Calphad Method, 2007.
[30] M. Hillert, L. Kjellqvist, H. Mao, M. Selleby, B. Sundman, Calphad 33 (2009) 227–232.
[31] S.E. Dorris, T.O. Mason, J. Am. Ceram. Soc. 71 (1988) 379–385.
[32] M. Keller, R. Dieckmann, Ber. Bunsenges. Phys. Chem. 89 (1985) 1095–1104.
[33] L. Kjellqvist, Doctoral Thesis, KTH, Stockholm, 2009.
[34] G. Inden, Z. Metallkd. 66 (1975) 577–582.
[35] M. Hillert, M. Jarl, Calphad 2 (1978) 227–238.
[36] J.R. Taylor, A.T. Dinsdale, Z. Metallkd. 84 (1993) 335–345.
[37] M. Tanahashi, N. Furuta, T. Taniguchi, C. Yamauchi, T. Fujisawa, ISIJ Int. 43 (2003) 7–13.
[38] I. Barin, Thermochemical Data of Pure Substances, 2nd ed., VCH Verlagsgesellschaft mbH, Weinheim, 1993.
[39] H.T. Tsai, A. Muan, J. Am. Ceram. Soc. 75 (1992) 1407–1411.
[40] L.M. Lenev, I.A. Novokhatskiy, Izv. Akad. Nauk SSSR, Metally 3 (1966) 73.
[41] O. Kubaschewski, C.B. Alcock, P.J. Spencer, Pergamon Press, New York, 1993.
[42] S. Dimitrov, A. Weyl, D. Janke, Steel Res. 66 (1995) 87.
[43] K.T. Jacob, G.N.K. Iyengar, W.K. Kim, J. Am. Ceram. Soc. 69 (1986) 487–492.
[44] K.T. Jacob, J. Electrochem. Soc. 125 (1978) 175–179.
[45] J.V. Biggers, Doctoral Thesis, Pennsylvania State University, 1966.
[46] J.M. Hastings, L.M. Corliss, Phys. Rev. 126 (1962) 556–565.
[47] D.H. Speidel, A. Muan, J. Am. Ceram. Soc. 46 (1963) 577–578.
[48] Y.V. Golikov, D.V. Bamburov, V.P. Barkhatov, V.F. Balakirev, J. Phys. Chem. Solids 46 (1985) 1357–1360.
[49] E. Pollert, P. Holba, M. Nevriva, J. Phys. Chem. Solids 38 (1977) 1145–1147.
[50] E. Pollert, M. Nevriva, J. Novak, Mater. Res. Bull. 15 (1980) 1453–1456.
[51] S. Geller, G.P. Espinosa, Phys. Rev. B 1 (1970) 3763–3769.
[52] A. Naoumidis, H.A. Schulze, W. Jungen, P. Lersch, J. Eur. Ceram. Soc. 7 (1991) 55–63.
[53] A.M. Garbers-Craig, R.J. Dippenaar, J. Am. Ceram. Soc. 81 (1998) 933–938.
[54] P. Holba, M. Nevriva, E. Pollert, Mater. Res. Bull. 10 (1975) 853–860.
[55] S. Ranghanthan, J.P. Hajra, Bull. Mater. Sci. 9 (1987) 149–158.
[56] A.P. Bobov, A.G. Zalazinsky, V.F. Balakirev, Y.V. Golikov, G.I. Chufarov, Zh. Fiz. Khim. 58 (1984) 750.
[57] M. Tanahashi, N. Furuta, C. Yamauchi, T. Fujisawa, ISIJ Int. 41 (2001) 1309–1315.
[58] A. Dinsdale, Calphad 15 (1991) 317–425.